



Single step synthesis and characterization of thermoresponsive hyaluronan hydrogels

Matteo D'Este*, Mauro Alini, David Eglin

AO Research Institute Davos, Clavadelstrasse 8, 7270 Davos, Switzerland

ARTICLE INFO

Article history:

Received 24 May 2012

Received in revised form 21 June 2012

Accepted 2 July 2012

Available online 14 July 2012

Keywords:

Hyaluronan

Poly(*N*-isopropylacrylamide)

Stimuli responsive hydrogel

ABSTRACT

An efficient and scale-up ready single-step synthesis for the conjugation of thermoresponsive polymers to hyaluronic acid (HA) was established. Jeffamines® (JFM) and poly(*N*-isopropylacrylamide) (PNIPAM) were grafted to HA via direct amidation mediated by 1,1'-carbonyldiimidazole activation. The temperature-induced gelation of the semi-synthetic co-polymers was characterized by rheology as a function of the temperature and by differential scanning calorimetry (DSC). A HA–JFM conjugate with sol–gel transition in a physiologically relevant temperature range was identified. The grafting of PNIPAM resulted in the drastic change of the main rheological properties of native HA, revealing the hydrophobic non-covalent nature of the interactions between the thermoresponsive brushes in the gel state. Owing to the reversibility of these interactions and the sharpness of the transition, the HA–PNIPAM conjugates are suitable candidates for the incorporation of drugs, cells or ceramic materials for different biomedical applications.

© 2012 Elsevier Ltd. All rights reserved.

1. Introduction

Stimuli responsive matrices are the archetype of “smart” biomaterials, and recently, they have been the subject of a great deal of research within the biomedical field. In particular, in situ forming hydrogels using an elevation of temperature between room to body temperature as a switch to increase their stiffness have been investigated for drug delivery systems (Coughlan, Quilty, & Corrigan, 2004; Klouda & Mikos, 2008; Liu, Shao, & Lü, 2006; Yin, Hoffman, & Stayton, 2006) and scaffolds in tissue engineering (Peroglio et al., 2011). Since its sharp transition occurs below body temperature, poly(*N*-isopropylacrylamide) (PNIPAM) is by far the most studied of the thermoresponsive polymers for biomedical applications. Owing to such features, numerous natural and synthetic polymers have been conjugated to PNIPAM to create thermoreversible hydrogels (Kim, Kim, & Jo, 2005; Liu, Shao, & Lü, 2006; Mortisen, Peroglio, Alini, & Eglin, 2010; Ohya, Nakayama, & Matsuda, 2004; Vasile & Nita, 2011; Yin, Hoffman, & Stayton, 2006). Hyaluronic acid (HA) plays a significant role within these polymers. It is ubiquitous, non-immunogenic, and a natural component of the extracellular matrix of various connective tissues with a key function in wound healing and the regeneration of these tissues. Hyaluronan grafted poly(*N*-isopropylacrylamide) (HA–PNIPAM) hydrogels were first reported

by Ohya, Nakayama, and Matsuda (2000). The synthesis was designed as the growth radical polymerization of PNIPAM brushes onto a HA backbone functionalized with a suitable chain transfer agent. This approach is not appropriate for controlling the molecular weight (MW) of the growing moiety. Moreover, the quasi-living photoradical-polymerization technique takes place in a free radical rich environment that has a degradative effect on the HA component. In other contributions from Ha et al. (2006), and more recently from Kazuaki, Ide, and Miyawak (2012), an amino terminated PNIPAM was conjugated to HA via amidation chemistry mediated by 1-ethyl-3-[3-dimethylaminopropyl] carbodiimide hydrochloride and *N*-hydroxysuccinimide (EDC + NHS), according to the method introduced by Bulpitt and Aeschlimann (1999). The opportunity to perform this conjugation chemistry in water makes it attractive, but in order to achieve a good degree of functionalization, a large excess of amine is required (Bulpitt & Aeschlimann, 1999). These previous investigations have described that the phase transition was detected via turbidimetry, but a shift in optical properties does not necessarily mean the transition from a flowing solution to a stiff gel. Rheometry or other mechanical testing techniques are more appropriate for measuring the performance of a temperature-responsive hydrogel. A further interesting approach utilizes the EDC + NHS chemistry to graft adipic dihydrazide to HA. In this approach, carboxy-terminated PNIPAM was grafted to the modified HA through an acyl-hydrazide group formation (Tan et al., 2009). The gel described within this paper was well characterized, but the weak mechanical properties achieved (elastic modulus in

* Corresponding author. Tel.: +41 81 414 24 53; fax: +41 81 414 22 88.
E-mail address: matteo.deste@aofoundation.org (M. D'Este).

the gel state <6 Pa) precludes its use in many applications. Moreover, a single step design for the synthesis would be desirable for scale up.

Recently, we reported a “click chemistry” synthesis for a HA–PNIPAM hydrogel (Mortisen et al., 2010; Peroglio et al., 2011). In this case, the reversible addition-fragmentation chain transfer polymerization (RAFT) synthesis of the PNIPAM brushes results in an extremely accurate control of the MW. Moreover this hydrogel is amenable for further derivatization with active species, such as drugs or growth factors. However, the synthesis procedure is not without drawbacks. In fact, the azido-terminated PNIPAM includes an enzymatically labile ester group. Besides, the alkyne-azide cycloaddition (AAC) grafting reaction is well known to be very efficient, but it needs the presence of Cu^I catalyst to be carried out at room temperature within the proper time scale. In terms of polysaccharides, and HA in particular, the presence of transition metals in water solution results in fast degradation. In fact, in presence of oxygen, a large variety of radical species are produced including the hydroxyl radical, which is a very aggressive species with the ability to efficiently depolymerize the polysaccharides (Soltes, Brezová, Stankovská, Kogan, & Gemeiner, 2006; Soltes, Stankovská, Brezová, Schiller, Arnhold, et al., 2006; Soltes et al., 2007). Since it is difficult to control the free-radical action, the copper catalyzed AAC “click chemistry” presents issues of reproducibility for this class of substrates. In fact, it has been reported that classic CuAAC leads to extensive degradation of polysaccharides (Lallana, Fernandez-Megia, & Riguera, 2009).

In order to overcome these drawbacks, we have developed an alternative single step amide formation on the carboxy-group of HA. The synthesis displays good inter batch reproducibility and is scale-up ready. A similar strategy has been reported for the grafting of small hydrophobic amines to HA (Bellini & Topai, 2000; Finelli, Chiessi, Galesso, Renier, & Paradossi, 2009). The coupling takes advantage of the 1,1'-carbonyldiimidazole (CDI) activation chemistry developed for the solid phase peptide synthesis, and to the best of our knowledge has never been used to the conjugation of polymeric or amphiphilic brushes to HA.

PNIPAM is by far the most extensively studied thermoresponsive polymer for use in biomedical applications. In order to verify the versatility of the conjugation technique proposed, we have applied the same protocol to another class of thermoresponsive polymers that is attracting increasing attention (Dulong, Mocanu, Picton, & Le Cerf, 2012; Mocanu, Mihaï, Dulong, Picton, & Lecerf, 2011; Mocanu, Mihaï, Dulong, Picton, & Le Cerf, 2012), i.e., Jeffamines® (JFMs). These polyethers are propylene oxide (PO)/ethylene oxide (EO) co-polymers, and their thermoresponsiveness depends upon the PO/EO ratio.

Products were characterized via hydrogen-1 nuclear magnetic resonance spectroscopy (¹H NMR), Fourier transform infra-red spectroscopy (FTIR), differential scanning calorimetry (DSC), and through rheology as a function of the temperature.

2. Experimental

2.1. Materials

HA Sodium salt from *Streptococcus equi* (HANa) was purchased from Contipro Biotech s.r.o. (Czech Republic). Two different batches of different MWs were used, specifically:

- High MW fraction (HMW), with weight-average molecular weight $M_w = 1506$ kDa and polydispersion index $M_w/M_n = 1.53$, where M_n indicates the number-average molecular weight.
- Low MW fraction (LMW), with $M_w = 293$ kDa and $M_w/M_n = 1.86$.

Amino-terminated poly(*N*-isopropylacrylamide) (PNIPAM-NH₂) of $M_n = 44 \pm 2.7$ kDa was purchased from Polymer Source, Inc. (CA). Amino-terminated JFMs were a gift of Huntsman GmbH (DE). All other reagents were purchased from Sigma–Aldrich (Switzerland); chemicals were of analytical grade at least, and were used without further purification.

2.2. Synthesis

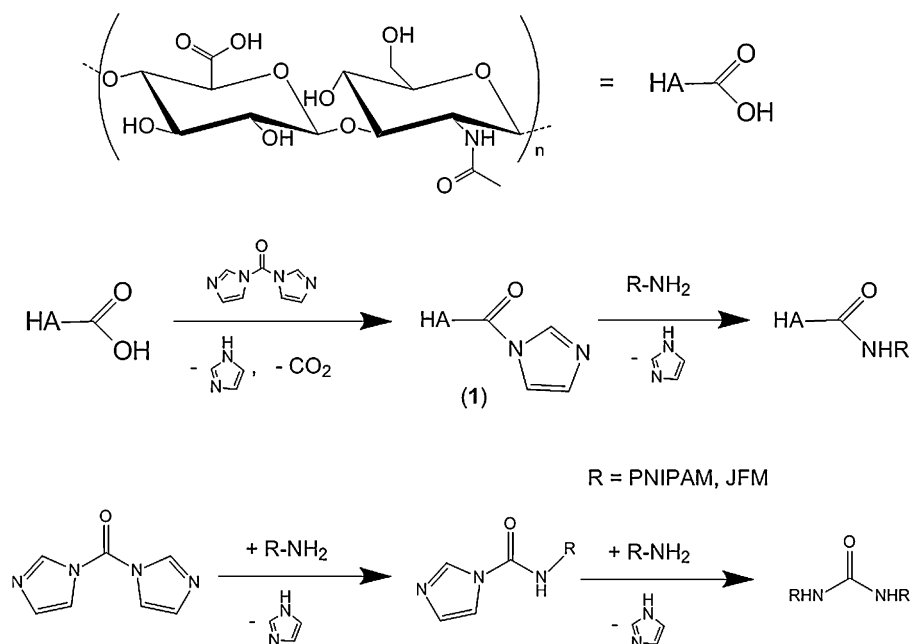
HANa of either HMW or LMW was transformed in its tetrabutylammonium salt (HATBA) via cationic exchange according to established procedures (Bellini & Topai, 2000). At room temperature, 2.0 g of HATBA were dissolved in 200 mL of dry dimethyl sulfoxide. The activation reaction to obtain the acyl-imidazole (**1**) was performed by addition of methanesulfonic acid and CDI, both equimolar to the repeating unit of HA (Scheme 1). Following 1 h of stirring, 3.7 g of thermoresponsive amino-terminated PNIPAM or JFM were added and stirred at room temperature. In the pre-hydrolyzed batches, 0.1% (v/v) of water was added just before the amino-terminated polymer addition. After 3 days, 10% (v/v) of saturated NaCl was slowly poured into the reaction solution and stirred 1 h before dialysis against demineralized water using regenerated cellulose dialysis tubes with nominal MW cut-off 50 kDa (Spectrapor no. 6, 34 mm flat width) for 5 days. Products were freeze-dried, desiccated under vacuum at 40 °C and stored at room temperature. The absence of chlorides in the final lyophile was assessed via Ag⁺ assay. In comparison, 3 batches of the conjugate HA–PNIPAM were synthesized via EDC/NHS chemistry, adapting the previously described procedure (Bulpitt & Aeschlimann, 1999). Briefly, 410 mg of HANa and 1.15 g of PNIPAM-NH₂ were dissolved in phosphate buffer. A 4-fold molar excess of EDC and NHS was added, and the pH set to 5.5, to foster the activation of HA. The pH was allowed rise to 7.2 ± 0.2 through NaOH addition after 1 h and the reaction was run to keep the pH within this range. This was run for a further 3 days and then the product was dialyzed against demineralized water and freeze-dried. The degree of functionalization was determined via NMR as described below.

2.3. Characterization

FT-IR analysis was performed on a Bruker Tensor 27 spectrophotometer equipped with a single reflection diamond attenuated total reflection (ATR) accessory. Freeze-dried HA–PNIPAMs or the as-received HANa powder was placed directly on the accessory. HANa/PNIPAM physical mixtures were dispersed in water, snap frozen in liquid nitrogen and lyophilized before analysis to obtain optimal sample uniformity. Spectra were acquired between 4000 and 500 cm^{−1} (average of 32 scans), and processed with the Opus 6.5 software.

DSC was performed on a Pyris DSC-1 Perkin-Elmer instrument calibrated with indium. PNIPAM-NH₂ and HA–PNIPAM solutions were weighed in hermetically closed aluminum pans. Measurements were carried out under a dry nitrogen atmosphere at a flow rate of 25 mL/min. Each cycle was run holding the sample 5 min at 10 °C, followed by a heating to 40 °C. Sample was held for 5 min at 40 °C and cooled at the initial temperature. Heating and cooling ramps were run at the rate of 5 or 0.5 °C/min. The reproducibility of the gelation and inverse transition was assessed by repeating the process for 30 cycles in the conditions described above, recording peak height and peak maximum or minimum.

¹H NMR analysis was performed on a Bruker Avance AV-500 NMR spectrometer using deuterium oxide as solvent without residual HOD peak suppression. Spectra were calibrated using 3-(trimethylsilyl)-1-propanesulfonic acid sodium salt as chemical shift internal standard, and processed with Mestrenova software.



Scheme 1. Conjugation of amino-terminated PNIPAM or JFM (R-NH₂) to HA via CDI chemistry, the formation of the *N*-acylimidazole (1) as active intermediate and the trapping of the amino-terminated polymer R-NH₂ via irreversible urea formation.

The MW distribution of HA was obtained by a modular multi-detector size exclusion chromatography (SEC) system consisting of an Alliance 2695 separation module (Waters, USA) equipped with two on-line detectors: a multi angle light scattering (MALS) Dawn DSP-F photometer (Wyatt, USA) and a 2414 differential refractometer (DRI) from Waters that was used as a concentration detector. Alignment of the different signals was implemented to correct the intrinsic temporal delay. Chromatographic specifications: two Shodex OHpak columns (KB806-KB805) from Showa Denko; mobile phase: 0.20 M NaCl; flow rate: 0.5 mL/min; temperature: 35 °C; injection volume: 150 µL; sample concentration: 0.2 or 0.8 mg/mL depending on the MW of the sample. The specific refractive index increment, dn/dc, with respect to the mobile phase was measured by a Chromatix KMX-16 differential refractometer.

The MW distribution for PNIPAM was obtained by an integrated multi-detector GPCV 2000 chromatographic system from Waters (USA). The GPCV 2000 system was equipped with three online detectors: (1) differential viscometer (DV); (2) differential refractometer (DRI) as a concentration detector; (3) additional MALS Dawn DSP-F photometer (Wyatt, USA). Alignment of the different signals was implemented to correct the intrinsic temporal delay. Chromatographic specifications: two PLgel Mixed C columns from Polymer Laboratories (UK); mobile phase: *N,N*-dimethylformamide (DMF)+0.1 M LiCl; flow rate: 0.8 mL/min; temperature: 50 °C; injection volume: 218.5 µL; sample concentration = 2 mg/mL.

Temperature-induced sol–gel transition was assessed with the vial inversion method for every batch. The synthesized conjugates were dissolved in phosphate buffer saline (PBS) pH = 7.4 at 10% (w/w) (HA–PNIPAM) or 10 and 20% (w/w) (HA–JFM) in hermetically closed vials. The flow-ability of the solutions was visually assessed at either room temperature (22 ± 2 °C) or at 37 °C after immersion on a thermostatic bath.

Rheological measurements were performed with a TA Instruments AR2000ex rheometer equipped with a Peltier controller and a plate–plate geometry, diameter 25 or 40 mm. The inertia of the system was calibrated before each measurement. The synthesized conjugates were dissolved in PBS (pH = 7.4) at 10% (w/w) (HA–PNIPAM) or 10 and 20% (w/w) (HA–JFM). Storage (or elastic) modulus (*G'*) and loss (or viscous) modulus (*G''*) were measured

as a function of the temperature. Solutions were subjected to a 5% oscillatory strain at 1 Hz while heating at 1 °C/min from 20 to 40 °C (to 50 °C for HA–JFMs). Low viscosity silicon oil was applied along the border of the plates after sample placement in order to avoid evaporation at the solution–atmosphere interface. The normal force control was used rather than constant gap, setting the force at 0.1 N (minimum value). Measurements were assessed to be in the viscoelastic linear region and verified through comparing the results with analogs runs performed at 2% strain. Mechanical spectra were measured at either 20 or 37 °C with the same modality, in the frequency range between 10^{−2} and 2 × 10² Hz.

3. Results and discussion

3.1. Synthesis of the conjugates

The synthetic procedure involves a first step where one imidazole ring condenses to the carboxy function of HA to form the active intermediate *N*-acylimidazole (1), which reacts directly with the amino terminated PNIPAM or JFM (Scheme 1). Given the sensitivity of the CDI and of the *N*-acylimidazole toward partially acidic protons the reaction is performed in a polar aprotic solvent, namely dimethyl sulfoxide. Then, the tetrabutylammonium rather than the Sodium salt of HA is used.

The potential of *N*-acylimidazoles in acylation chemistry was recognized in the early 1950s, and the use of CDI for their preparation was introduced a few years later (Paul & Anderson, 1960; Staab, 1957). The main restriction to the use of CDI and analogs in organic synthesis is the sensitivity to moisture, which is not displayed by other condensing agents such as carbodiimides (Joachim, 2007). However, the improved efficiency, minimal racemization, ease of purification and harmlessness of the by-products CO₂ and imidazole makes the use of CDI a valid synthetic tool for specific applications.

In order to assess the robustness of the process, we have compared the efficiency of the synthesis in “dry” and “humid” conditions. Table 1 displays the degree of substitution (DS) for different batches with or without the addition of water. In particular, Batches 1 and 2, prepared via the standard procedure without

Table 1

DS (mol%) for different batches of conjugate HA–PNIPAM. Batches with the asterisk (*) were pre-hydrolyzed with water (see Section 3.1). Methods A and B refer to different integration of the ^1H NMR spectra (see Section 3.2.1).

Batch ID	DS (mol/mol, %)	
	Method A	Method B
1	6.6	6.4
2	7.5	7.4
3*	5.9	5.6
4*	7.0	7.0

pre-hydrolysis; batches 3 and 4, (marked with (*)), where water was added to the reaction solution during amine addition to realize a concentration of 0.1% (w/v) that corresponded to 4 moles H_2O per mole of HA dimer.

Water could potentially improve or reduce the reaction efficiency via two different mechanisms acting in opposite directions. A water-free environment helps to avoid the hydrolysis of the reactive intermediate, improving the amidation efficiency. Furthermore, small amounts of water when added just prior to the amino compound can hydrolyze the CDI that did not react with the carboxyls. If the excess of CDI was not eliminated, then it would eventually react with the amine to form an isocyanate (Scheme 1) that subsequently trapped by another amine equivalent to yield a derivative of urea that would sequester irreversibly the amino-terminated polymer and impede the subsequent amidation (Joachim, 2007). In our case, both mechanisms are probably active, and their competition makes the overall process independent from the presence of small amounts of water (Table 1). In fact, whilst the pre-hydrolyzed batches displayed systematically lower substitution, such differences were not considered significant due to the intrinsic error within the integration procedure, as pointed out in Section 3.2.1.

The grafting of amphiphilic brushes to the polysaccharide via direct amidation was effective and efficient. The grafting is reproducible, although not quantitative. In general, the non-quantitative grafting is a common feature of reactions involving HA and biopolymers. In fact, the well consolidated coupling of amines with HA via EDC+NHS requires massive excess of the amine (Bulpitt & Aeschlimann, 1999). If scaled-up, this procedure is not justifiable in terms of chemical waste production and economically unsustainable if the amine is expensive. In comparison, we have synthesized HA–PNIPAM via EDC+NHS chemistry using the same feed ratio employed for the CDI chemistry. The DS obtained was about one half (data not shown), and the resulting solution did not display sol–gel transition upon vial inversion after heating.

3.2. Characterization of HA–PNIPAMs conjugates

3.2.1. Solution properties and spectrometric analysis

A first indication of the chemical ligation between HA and PNIPAM was given by the physical appearance of the solution. Despite the water solubility of both polymers, the dispersion of HA and PNIPAM in PBS at pH = 7.4 resulted in a marked phase separation. Solutions of the conjugate when kept at room temperature or lower created a clear homogeneous solution, with low viscosity at a relatively high concentration (10–15%, w/w).

In order to optimize the design of the co-polymer the influence of the HA backbone length on the mechanical properties of the hydrogel has been studied, comparing HA–PNIPAM from both HA HMW and LMW.

The MW of the PNIPAM brushes is fundamental for controlling the temperature induced sol–gel transition. High MWs are associated with a wider and sharper transition, but also with shrinking features that might compromise the use of the material as a cell

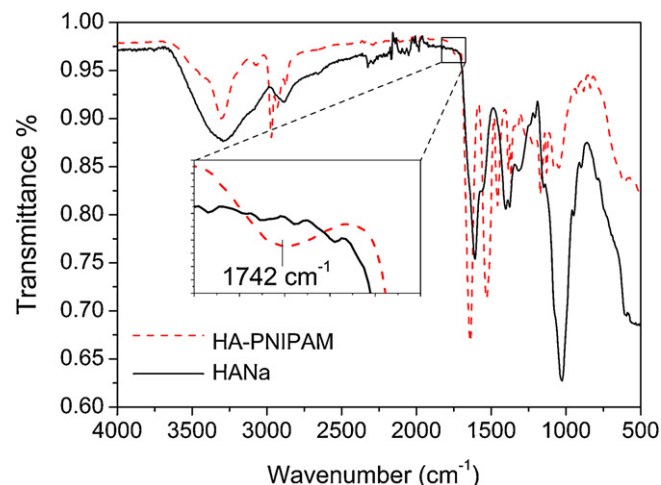


Fig. 1. FT-IR spectrum of HANa salt and its conjugate with PNIPAM. The inset shows the spectral feature characteristic of the conjugate and not present on the HA, PNIPAM and their mixture.

carrier (Mortisen et al., 2010). In the present study, PNIPAM brushes of MW = 44 kDa (determined via absolute SEC) have been selected in order to optimize gelation and cell carrier capability.

The FTIR spectrum of the HA–PNIPAM conjugate displays a shift in the carbonyl stretching from 1605 cm^{-1} for the underivatized HA to about 1640 cm^{-1} for the conjugate, in addition to a shift for the bands at 1404 cm^{-1} and 1376 cm^{-1} to 1386 cm^{-1} and 1366 cm^{-1} , respectively (Fig. 1). This feature is usually attributed in the literature to the amide bond formation between HA and PNIPAM. In order to verify this hypothesis, we have compared the FTIR spectra of physical mixtures of HA and PNIPAM non-chemically conjugated, in the weight ratio HA/PNIPAM between 0.5 and 4.0. In fact, the band appearing at 1640 cm^{-1} is a linear combination of the signals arising from the pristine polymers, and is not attributable to the new amide bond formation. This new amide is in fact stoichiometrically marginal, as both PNIPAM and HA on their own have an amide bond for each repeating unit. The only spectral feature not present in the pristine polymers and their physical mixtures, demonstrating the conjugation was a small peak around 1742 cm^{-1} (inset in Fig. 1). As illustrated in Scheme 1, the formation of the imidazolide active intermediate of HA was performed in acidic environment, with the carboxy groups in the non-dissociated form. Hence, in the final product some carboxylic functions of HA may be present in acidic form. In order to verify this eventuality, we have compared the FTIR spectrum of the PNIPAM conjugate with the same specimen after alkaline treatment with NaOH. The spectra were almost identical, confirming that the HA carboxy functions in the conjugate were present as carboxylate.

Similarly to FTIR, the ^1H NMR spectrum corresponds to the sum of the polymeric components of the semi-synthetic conjugate (Fig. 2). The ligation does not give rise to any new resonance situated in a spectral region free of other signals, so conventional ^1H NMR spectroscopy cannot be used as direct proof of the chemical ligation. HA characteristic signals are the singlet at 2.01 ppm and a broad multiplet between 3.2 and 3.7 ppm, assigned to most of the protons directly bounded to the ring. PNIPAM gives a sharp singlet at 1.14 ppm due to methyl groups in the *iso*-propyl moiety; the proton connected to the tertiary carbon in the same functional group gives resonance at 3.89 ppm, superimposing to signals from HA. Interestingly, the aliphatic protons marked as “d” in Fig. 2 give a split signal. This feature is attributed to the slow rotation along the axis through the c–d carbon atoms, determined by the steric hindrance of the pending moiety, or its involvement in hydrogen bonding. The slow rotation let the protons (“d”) to detect different

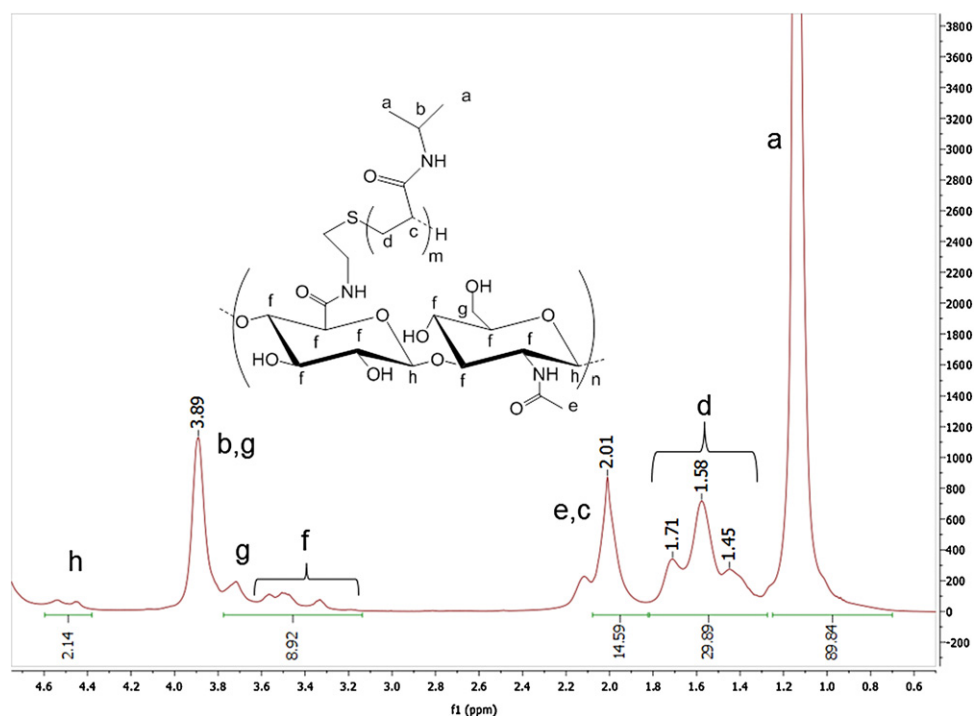


Fig. 2. ^1H NMR spectrum of the conjugate HA-PNIPAM.

chemical surroundings, making them chemically non-equivalent. This feature was also observed in the spectrum of pure PNIPAM in D_2O (not shown), and the interpretation is confirmed by the broadness of the signals. Despite the overlap of some key spectral features (e.g., the *N*-acetyl of HA and one aliphatic proton from the PNIPAM backbone “e” and “c” in Fig. 2 were detected at exactly 2.01 ppm), it was possible to calculate the DS. Two different methods have been employed: integration of the peaks of HA at 3.00–3.77 ppm (integrating for 9 HA protons, as verified by integration of pristine HA) and PNIPAM at 1.14 ppm (Method A), or integration of the peak at 2.01 ppm (both polymers) after subtraction of the HA measured from the 3.00 to 3.77 ppm multiplet integrating for 9 protons (Method B). Table 1 compares the molar DS (%) calculated through the two methods for different batches. Results are in agreement within the experimental error (estimated to be no less than 10%). Table 1 is also representative of the range of DS displayed for different batches, that resulted $6.5 \pm 1.0\%$ in moles. By modification of the feeding ratio and other conjugation conditions, it was possible to verify that conjugates with a DS below 5.5% do not display appropriate gelation upon temperature increase, as verified via vial inversion method.

3.2.2. Rheology of the HA-PNIPAM conjugate

Rheometry is a suitable technique for investigating phase transitions in thermoresponsive hydrogels for their potential application as cell carriers and drug delivery systems. Moreover, comparing the viscoelastic profiles of the conjugate and the native polymers, it is possible to gain an insight into the underlying molecular structure in solution. Viscoelasticity of the conjugates was measured upon independent variations of temperature and frequency.

Viscoelastic shear moduli of 10% (w/w) solutions of the conjugate in PBS are displayed in Fig. 3 as a function of temperature. Conjugates prepared from HMW (1.50 MDa, continuous lines) and LMW HA (0.29 MDa, dotted lines) were compared. At room temperature, no viscoelasticity was displayed, with G' and $G'' \cong 1$ Pa. As the temperature increased above 30°C , the systems lose their flowability, and viscoelastic shear moduli rise by 2–3 orders of magnitude in

a temperature range of less than 2°C . Moreover, the passage from the regime of loss modulus prevalence ($G'' > G'$) to the regime of storage modulus prevalence ($G' > G''$) was observed.

The transition profile is independent of the MW of the HA backbone. The underlying molecular interpretation of this non-dependency is different for the sol and the gel state. In the gel state above the transition temperature, the viscoelasticity observed is due to non-covalent hydrophobic interactions between the PNIPAM brushes. If the entanglement between the HA backbone chains would play a role (as in underivatized HA), then the viscoelasticity in the gel state would depend on its MW. Hence, the non-dependency observed is an indicator of the structural role of the non-covalent PNIPAM interactions as the crosslinks are responsible for the elasticity of the gel structure.

In the sol state, HA-PNIPAM in PBS displays a dramatically lower viscoelasticity compared to underivatized HA, with G' and G'' equal,

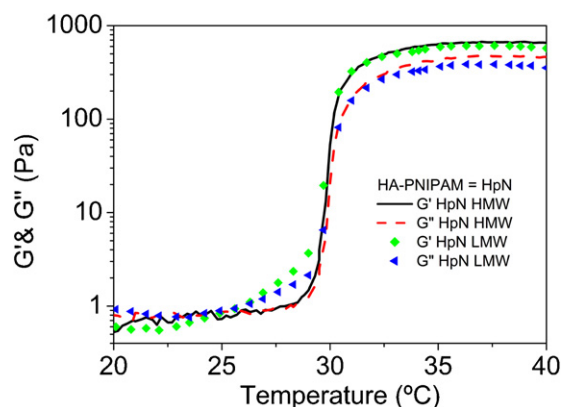


Fig. 3. Viscoelastic shear moduli of a 10% (w/w) solution of HA-PNIPAM in PBS at 1 Hz as function of the temperature. Continuous lines refer to conjugates from high molecular weight (HMW) haluronan, dotted lines conjugate from low molecular weight (LMW) HA.

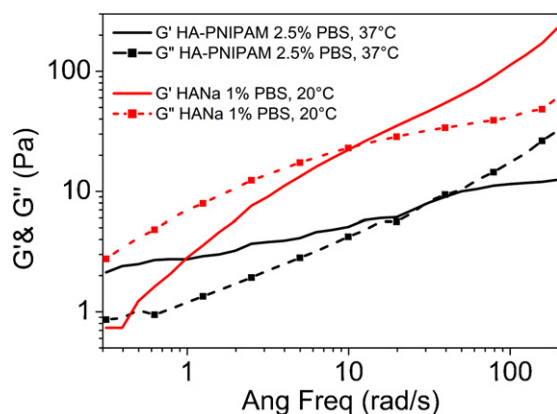


Fig. 4. Mechanical spectrum of HANA at 20 °C and concentration 1% (w/w) in PBS (red lines) compared with HA-PNIPAM at 2.5% (w/w) in PBS and 37 °C (black lines). Straight lines refer to the storage modulus, dashed lines with squares superimposed refer to the loss modulus. (For interpretation of the references to color in this figure legend, the reader is referred to the web version of the article.)

respectively, to 9304 Pa and 2826 for HANA, and 0.38 Pa and 0.70 Pa for HA-PNIPAM10% (w/v) solutions at 25 °C. In the sol state, the viscoelasticity of HA in solution is attributed to the stiffness of its chains and their interactions, mainly via hydrogen bonding and hydrophobic interactions (Hardingham, 2004). PNIPAM moieties have an amide bond for each repeating unit, and the amide group can act as either a hydrogen bond acceptor (carbonyl group) or hydrogen bond donor (the proton in the NH group). Moreover, the isopropyl group is a hydrophobic domain able to disrupt hydrophobic interactions between the HA chains. Thus, the PNIPAM grafted to HA is able to perturb the architecture of interactions between the HA chains, leading to the observed dramatic decrease of viscoelasticity. If HA chains are not interacting in solution, then the viscoelasticity observed results are independent of their MW.

This interpretation was confirmed by the mechanical spectrum of the conjugate solutions at physiological temperature (Fig. 4). The graph shows the frequency dependence of the dynamic shear moduli for the HA-PNIPAM hydrogel at 37 °C and concentration of 2.5% (w/w) in PBS (pH = 7.4), and compared to a 1% (w/w) solution of HA in the same solvent. In the case of the underivatized HA solution, a crossover point with viscous prevalence at low frequency was observed. This behavior is essential for the lubrication and mechanical protection of cartilage within the synovial joints under different dynamic regimes. The observed profile is a consequence of the interactions between the HA chains (Hardingham, 2004). In terms of the conjugate, a crossover point was also observed, but in this case the storage modulus is dominant at low frequencies. Since in the gel state at 37 °C the crosslinking is defined by weak hydrophobic interactions between the PNIPAM brushes, as the frequency of mechanical energy input increases this weak network is broken, and the solution displays a viscous prevalence.

To summarize, the results obtained from the different rheological techniques used to characterize the conjugate, are consistent, and confirm that the structure of the gel is supported by the reversible non-covalent entanglement between the PNIPAM moieties rather than dynamical interactions among the HA chains in solution. The sharpness and the physiologically relevant temperature of transition make the conjugate a suitable candidate for biomedical applications.

3.2.3. DSC analysis of the HA-PNIPAM conjugate

DSC is a convenient technique to study the sol–gel transition of solutions of the HA-PNIPAM conjugate upon cycles of

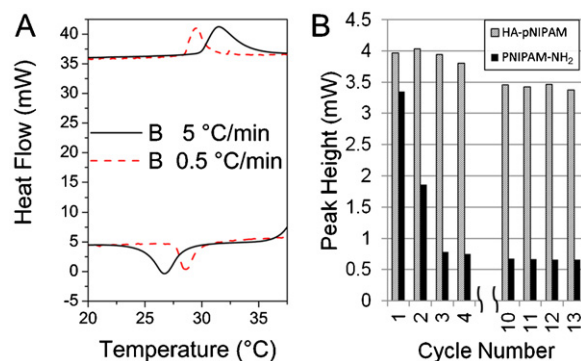


Fig. 5. Reversibility of HA-PNIPAM gelation. (A) DSC thermogram for HA-PNIPAM 10% (w/w) in PBS. Curves representing the first cycle at the heating rate indicated. (B) Peak height (mW) for the gel–sol transition as function of the cycle number for PNIPAM-NH₂ and its conjugate with HA. While for PNIPAM the peak height is reduced by a factor 4 at the third cycle, the conjugate with HA displays only a slight decrease over 13 cycles.

heating–cooling. Moreover, unlike rheology, DSC is performed within hermetically closed pans, and then it is more suitable to characterize the phase transition upon reiteration of several heating–cooling sequences.

During a heating ramp, the passage to the gel state was observed as endothermic first order transition (Fig. 5A). The temperature corresponding to the peak maximum was consistent with the transition temperature observed via rheological analysis. In a typical cycle, the transition temperature observed during the heating ramp was higher than the transition temperature for the cooling ramp (Fig. 5A). The amplitude of the hysteresis was 4.3 °C at a heating rate of 5 °C/min (continuous line), and 2.0 °C, if the rate was reduced to 0.5 °C/min (dashed line). The rate-dependency indicates that the hysteresis depends upon kinetic-non-equilibrium phenomena.

The reversibility of the sol–gel transition is a key feature concerning the use of the conjugate as hydrogel scaffold in tissue engineering. In fact, in a typical cell therapy protocol, cells need to be easily mixed within the matrix (room temperature, sol state) and expanded at physiological temperature (gel state). Then, the reversibility of the gelation process can be used to bring the construct back to the fluid state, allowing an easy injection without high mechanical stress in order to preserve cell viability, easy integration into the surrounding tissues but also no systemic spreading owing to the temperature promoted gelation.

The maximum variation of transition temperature observed within 30 heating–cooling cycles was 0.15 °C for the transition to the gel state and 0.10 °C for the transition from the gel to the fluid state. Such a small variation is indicative of the reversibility of the gelation process. Another measure of the reproducibility of the thermal cycles is the peak height, measured as the gap to the baseline. Peak height has been chosen rather than the transition enthalpy because the last is less objective, depending critically on the integration boundaries. Fig. 5B displays the peak height for the cooling ramp as a function of the cycle number for the gel–sol transition of PNIPAM and its conjugate with HA. While at the third cycle PNIPAM reaches a plateau with height about 20% of the value presented for the first cycle, the conjugate with HA displays a much smaller difference, reaching a plateau at a value approximately 85% of the first cycle after 10 cycles. As observed in our previous paper (Mortisen et al., 2010), the conjugation with HA improves the reproducibility of the thermal cycles of the thermoresponsive PNIPAM.

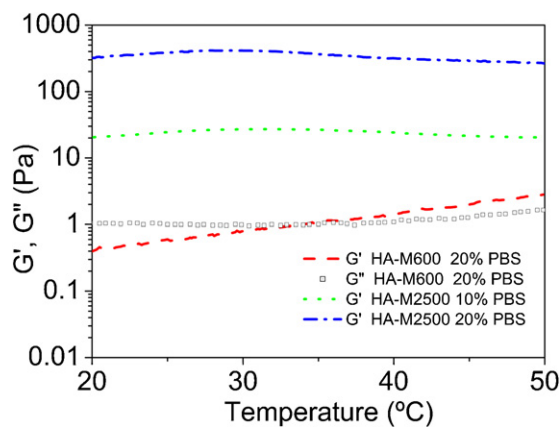


Fig. 6. Viscoelastic shear moduli of the HA-JFM conjugates as function of the temperature. Only the derivative with JFM M-600 displayed stiffness increase with the temperature.

3.2.4. Synthesis and characterization of the derivatives with Jeffamines®

In order to prove the effectiveness and versatility of the synthesis scheme illustrated, JFMs were conjugated with HA using the same synthetic strategy. JFMs are available with different hydrophilicity as determined by the PO/EO ratio and with various end functional groups. In order to compare with the PNIPAM derivatives previously described, we have used mono-amine JFMs with relatively high PO content to emphasize the amphiphilic and thermoreversible characteristic, namely:

- JFM M-600, featured by MW equal to 0.6 kDa and ratio PO/EO = 9/1, and
- JFM M-2005 of MW equal to 2 kDa and ratio PO/EO = 29/6

In both JFMs cases, the conjugations were performed to reproduce the same weight feed ratio adopted for the PNIPAM derivatives. ^1H NMR spectra of the derivatives displayed the features of both polymers, with the characteristic peak of the acetyl protons of HA at 2.01 ppm, and the methyl protons of the PO at 1.15 ppm. The ratio between these signals allowed the determination of the degree of functionalization. All the other aliphatic protons were superimposed in a broad multiplet between 3.0 and 4.0 ppm circa. The DS values are 20% for the M-2005 derivative and 29% for the M-600 derivative, reflecting the largest excess in moles used for the lower MW JFM, and its improved mobility and capacity to reach and react with HA. The temperature-promoted sol-gel transition was investigated via oscillatory rheology, measuring the shear dynamic moduli at the frequency of 1 Hz as a function of the temperature. Only the derivative with JFM M-600 displayed an increase in storage modulus upon temperature increase (Fig. 6), with a gelation point at 35 °C, in a physiologically relevant temperature. This result is in accordance with the highest DS achieved for this conjugate, but it might also depend upon the different hydrophobicity of the brushes. In fact, there are reports in the literature that show for this class of co-polymers, that the ΔH of the phase transition depends upon the PO rather than the EO content (Mitchard et al., 1992), and PO content is higher for M-600 compared with M-2005. The transition is not very pronounced, the elastic modulus increasing of 1 order of magnitude in the temperature range between 20 and 50 °C. A further fundamental parameter influencing the phase transition of thermoresponsive polymers and co-polymers is their MW. The low gradient of the transition can be caused by the low MW of the amphiphilic brushes. Unfortunately, the non-availability of higher analogs of JFMs with identical

composition did not allow us to investigate the influence of this important feature.

4. Conclusions

A convenient route to the grafting of amphiphilic polymers to HA has been presented. Despite its intrinsic sensitivity to moisture, the CDI has proven to be a suitable activator of HA toward coupling chemistry via amide formation. The reaction efficiency was independent of the addition of a 4-fold molar excess of water (as ratio to the HA repeating unit), revealing the robustness of the procedure toward environmental variables and inter-batch reproducibility. The method is versatile and scale-up ready, as demonstrated by the conjugation of PNIPAM and JFMs. Conjugates HA-JFMs were obtained from JFMs of different MW and hydrophobicity. The derivative with JFM M-600, characterized by a higher DS and higher hydrophobicity displayed temperature induced sol-gel transition in a physiologically relevant range. The low gradient of the transition restrains the possible applications for this compound, but the properties of its analogs prepared from JFM with the same composition and higher MW need to be investigated.

PNIPAM conjugates with a DS of 6.5 ± 1 mol% exhibited the best performance in terms of temperature-induced sol-gel transition, with a wider jump of viscoelasticity in a narrower temperature range, below body temperature. Rheological characterization of PBS solutions of these compounds presented opposite behavior when compared to that of underivatized HA concerning viscosity at room temperature and mechanical spectrum. Thus, revealing the disruption of the interactions between the chains of HA in the flowing solution state and the non-covalent nature of the entanglement in the gel state. The reversibility of this non-covalent interaction was investigated in more depth via DSC analysis, demonstrating a high reproducibility over 30 cycles of heating-cooling. The reversible and non-covalent nature of the hydrogel makes it an ideal candidate for the incorporation of drugs, biological drugs, cells or bio-ceramics particles for applications as drug delivery system and in tissue engineering.

Acknowledgments

Dr. Carole Boissard and Dr. Pierre-Etienne Bourban (EPFL, Lausanne) are sincerely acknowledged for the possibility of conducting extensive rheological measurements; Prof. M. Textor and Mrs. D. Sutter from ETH Zurich (Switzerland) are acknowledged for permitting and performing NMR analysis, respectively. We express thanks also to Huntsman GmbH (DE) for the gift of amino-terminated JFMs, to Dr. Raniero Mendichi for the SEC analysis, to Markus Glarner for assistance in the chemical synthesis and to Dr. Girish Patappa for the critical revision of the manuscript. The research leading to these results has received funding from the European Union's 7th Framework Program under grant agreement no. NMP3-SL-2010-245993.

References

- Bellini, D., & Topai, A. (2000, January 13). *Amides of hyaluronic acid and the derivatives thereof and a process for their preparation*. Patent Num WO0001733 (A1).
- Bulpitt, P., & Aeschlimann, D. (1999). New strategy for chemical modification of hyaluronic acid: Preparation of functionalized derivatives and their use in the formation of novel biocompatible hydrogels. *Journal of Biomedical Materials Research*, 47, 152–169.
- Coughlan, D. C., Quilty, F. P., & Corrigan, O. I. (2004). Effect of drug physicochemical properties on swelling/deswelling kinetics and pulsatile drug release from thermoresponsive poly(*N*-isopropylacrylamide) hydrogels. *Journal of Controlled Release*, 98, 97–114.
- Dulong, V., Mocanu, G., Picton, L., & Le Cerf, D. (2012). Amphiphilic and thermosensitive copolymers based on pullulan and Jeffamine®: Synthesis, characterization and physicochemical properties. *Carbohydrate Polymers*, 87, 1522–1531.

- Finelli, I., Chiessi, E., Galesso, D., Renier, D., & Paradossi, G. (2009). Gel-like structure of a hexadecyl derivative of hyaluronic acid for the treatment of osteoarthritis. *Macromolecular Bioscience*, 9, 646–653.
- Ha, D. I., Lee, S. B., Chong, M. S., Lee, Y. M., Kim, S. Y., & Park, Y. H. (2006). Preparation of thermo-responsive and injectable hydrogels based on hyaluronic acid and poly(*N*-isopropylacrylamide) and their drug release behaviors. *Macromolecular Research*, 14, 87–93.
- Hardingham, T. (2004). Chapter 1. Solution properties of hyaluronan. In G. G. Hari, & A. H. Charles (Eds.), *Chemistry and biology of hyaluronan* (pp. 1–19). Oxford: Elsevier Science, Ltd.
- Joachim, P. (2007). *Synthesis of aldehydes by oxidation. Science of Synthesis: Houben–Weyl Methods of Molecular Transformation. Category 4. Compounds with two carbon-heteroatom bonds. Vol. 25. Aldehydes and heteroatom analogues*. Stuttgart: Georg Thieme Verlag, pp. 25–56.
- Kazuaki, M., Ide, M., & Miyawak, F. (2012). Biological evaluation of tissue-engineered cartilage using thermoresponsive poly(*N*-isopropylacrylamide)-grafted hyaluronan. *Journal of Biomaterials and Nanobiotechnology*, 3, 1–9.
- Kim, K. H., Kim, J., & Jo, W. H. (2005). Preparation of hydrogel nanoparticles by atom transfer radical polymerization of *N*-isopropylacrylamide in aqueous media using PEG macro-initiator. *Polymer*, 46, 2836–2840.
- Kloda, L., & Mikos, A. G. (2008). Thermoresponsive hydrogels in biomedical applications. *European Journal of Pharmaceutics and Biopharmaceutics*, 68, 34–45.
- Lallana, E., Fernandez-Megia, E., & Riguera, R. (2009). Surpassing the use of copper in the click functionalization of polymeric nanostructures: A strain-promoted approach. *Journal of the American Chemical Society*, 131, 5748–5750.
- Liu, Y., Shao, Y., & Lü, J. (2006). Preparation, properties and controlled release behaviors of pH-induced thermosensitive amphiphilic gels. *Biomaterials*, 27, 4016–4024.
- Mitchard, N. M., Beezer, A. E., Mitchell, J. C., Armstrong, J. K., Chowdhry, B. Z., Leharne, S., et al. (1992). Thermodynamic analysis of scanning calorimetric transitions observed for dilute aqueous solutions of ABA block copolymers. *The Journal of Physical Chemistry*, 96, 9507–9512.
- Mocanu, G., Mihai, D., Dulong, V., Picton, L., & Lecerf, D. (2011). New anionic amphiphilic thermosensitive pullulan derivatives. *Carbohydrate Polymers*, 84, 276–281.
- Mocanu, G., Mihai, D., Dulong, V., Picton, L., & Le Cerf, D. (2012). New anionic crosslinked multi-responsive pullulan hydrogels. *Carbohydrate Polymers*, 87, 1440–1446.
- Mortisen, D., Peroglio, M., Alini, M., & Eglin, D. (2010). Tailoring thermoreversible hyaluronan hydrogels by click chemistry and RAFT polymerization for cell and drug therapy. *Biomacromolecules*, 11, 1261–1272.
- Ohya, S., Nakayama, Y., & Matsuda, T. (2000). Artificial extracellular matrix design in tissue engineering: Synthesis of thermoresponsive hyaluronic acid and its supramolecular organization. *Japan Journal of Artificial Organs*, 29, 446–451.
- Ohya, S., Nakayama, Y., & Matsuda, T. (2004). In vivo evaluation of poly(*N*-isopropylacrylamide) (PNIPAM)-grafted gelatin as an in situ-formable scaffold. *Journal of Artificial Organs*, 7, 181–186.
- Paul, R., & Anderson, G. W. (1960). *N,N'*-Carbonyldiimidazole, a new peptide forming reagent. *Journal of the American Chemical Society*, 82, 4596–4600.
- Peroglio, M., Grad, S., Mortisen, D., Sprecher, C., Illien-Jünger, S., Alini, M., et al. (2011). Injectable thermoreversible hyaluronan-based hydrogels for nucleus pulposus cell encapsulation. *European Spine Journal*, 1–11.
- Soltes, L., Brezová, V., Stankovská, M., Kogan, G., & Gemeiner, P. (2006). Degradation of high-molecular-weight hyaluronan by hydrogen peroxide in the presence of cupric ions. *Carbohydrate Research*, 341, 639–644.
- Soltes, L., Stankovská, M., Brezová, V., Schiller, J., Arnhold, J., Kogan, G., et al. (2006). Hyaluronan degradation by copper(II) chloride and ascorbate: Rotational viscometric, EPR spin-trapping, and MALDI-TOF mass spectrometric investigations. *Carbohydrate Research*, 341, 2826–2834.
- Soltes, L., Valachová, K., Mendichi, R., Kogan, G., Arnhold, J., & Gemeiner, P. (2007). Solution properties of high-molar-mass hyaluronans: The biopolymer degradation by ascorbate. *Carbohydrate Research*, 342, 1071–1077.
- Staab, H. A. (1957). Reaktionsfähige heterocyclische diamide der Kohlensäure. *Justus Liebigs Annalen der Chemie*, 609, 75–83.
- Tan, H., Ramirez, C. M., Miljkovic, N., Li, H., Rubin, J. P., & Marra, K. G. (2009). Thermosensitive injectable hyaluronic acid hydrogel for adipose tissue engineering. *Biomaterials*, 30, 6844–6853.
- Vasile, C., & Nita, L. E. (2011). Novel multi-stimuli responsive sodium alginate-grafted-poly(*N*-isopropylacrylamide) copolymers. II. Dilute solution properties. *Carbohydrate Polymers*, 86, 77–84.
- Yin, X., Hoffman, A. S., & Stayton, P. S. (2006). Poly(*N*-isopropylacrylamide-co-propylacrylic acid) copolymers that respond sharply to temperature and pH. *Biomacromolecules*, 7, 1381–1385.